



HAL
open science

Investigation of lithium distribution in the rat brain ex vivo using lithium-7 magnetic resonance spectroscopy and imaging at 17.2 T

Jacques Stout, Anne-Sophie Hanak, Lucie Chevillard, Boucif Djemaï, Patricia Risède, Eric Giacomini, Joël Poupon, David André Barrière, Frank Bellivier, Bruno Mégarbane, et al.

► To cite this version:

Jacques Stout, Anne-Sophie Hanak, Lucie Chevillard, Boucif Djemaï, Patricia Risède, et al.. Investigation of lithium distribution in the rat brain ex vivo using lithium-7 magnetic resonance spectroscopy and imaging at 17.2 T. *NMR in Biomedicine*, 2017, 30 (11), pp.e3770. 10.1002/nbm.3770 . hal-03822913

HAL Id: hal-03822913

<https://hal.science/hal-03822913>


Submitted on 9 Dec 2022

HAL is a multi-disciplinary open access archive for the deposit and dissemination of scientific research documents, whether they are published or not. The documents may come from teaching and research institutions in France or abroad, or from public or private research centers.

L'archive ouverte pluridisciplinaire **HAL**, est destinée au dépôt et à la diffusion de documents scientifiques de niveau recherche, publiés ou non, émanant des établissements d'enseignement et de recherche français ou étrangers, des laboratoires publics ou privés.

RESEARCH ARTICLE

Investigation of lithium distribution in the rat brain *ex vivo* using lithium-7 magnetic resonance spectroscopy and imaging at 17.2 T

Jacques Stout¹ | Anne-Sophie Hanak² | Lucie Chevillard² | Boucif Djemaï¹ |
Patricia Risède² | Eric Giacomini¹ | Joël Poupon³ | David André Barrière^{1,4} |
Frank Bellivier^{2,5} | Bruno Mégarbane^{2,6} | Fawzi Boumezbear¹ 

¹NeuroSpin, Institut Frédéric Joliot, CEA, Université Paris-Saclay, Gif-sur-Yvette, France

²Inserm UMR-S 1144, Universités Paris-Descartes & Paris-Diderot, Paris, France

³APHP, GH Saint-Louis-Lariboisière-Fernand Widal, Laboratoire de Toxicologie biologique, Paris, France

⁴Inserm UMR-S 894, Université Paris-Descartes, Paris, France

⁵APHP, GH Saint-Louis-Lariboisière-Fernand Widal, Département de Psychiatrie et de Médecine Addictologique, Paris, France

⁶APHP, GH Saint-Louis-Lariboisière-Fernand Widal, Réanimation Médicale et Toxicologique, Paris, France

Correspondence

F. Boumezbear, NeuroSpin, ISVFJ, CEA, Centre de Saclay, Bât. 145, 91191 Gif-sur-Yvette Cedex, France.
Email: fawzi.boumezbear@cea.fr

Funding information

Agence Nationale de la Recherche, Grant/Award Number: BIP-Li7 / ANR-14-CE15-0003-01; IDEX Université Sorbonne-Paris-Cité, Grant/Award Number: RespoLi project 2013

Lithium is the first-line mood stabilizer for the treatment of patients with bipolar disorder. However, its mechanisms of action and transport across the blood–brain barrier remain poorly understood. The contribution of lithium-7 magnetic resonance imaging (⁷Li MRI) to investigate brain lithium distribution remains limited because of the modest sensitivity of the lithium nucleus and the expected low brain concentrations in humans and animal models. Therefore, we decided to image lithium distribution in the rat brain *ex vivo* using a turbo-spin-echo imaging sequence at 17.2 T. The estimation of lithium concentrations was performed using a phantom replacement approach accounting for B_1 inhomogeneities and differential T_1 and T_2 weighting. Our MRI-derived lithium concentrations were validated by comparison with inductively coupled plasma-mass spectrometry (ICP-MS) measurements ($[Li]_{MRI} = 1.18[Li]_{MS}$, $R = 0.95$). Overall, a sensitivity of 0.03 mmol/L was achieved for a spatial resolution of 16 μ L. Lithium distribution was uneven throughout the brain (normalized lithium content ranged from 0.4 to 1.4) and was mostly symmetrical, with consistently lower concentrations in the metencephalon (cerebellum and brainstem) and higher concentrations in the cortex. Interestingly, low lithium concentrations were also observed close to the lateral ventricles. The average brain-to-plasma lithium ratio was 0.34 ± 0.04 , ranging from 0.29 to 0.39. Brain lithium concentrations were reasonably correlated with plasma lithium concentrations, with Pearson correlation factors ranging from 0.63 to 0.90.

KEYWORDS

⁷Li NMR, brain, distribution, quantification, ultra-high magnetic field

1 | INTRODUCTION

Bipolar disorder (BD) is a major affective disorder affecting 1–4% of the general population, associated with considerable burden and costs.¹ Lithium (Li) is the most frequently recommended mood stabilizer treatment and has also been shown to efficiently prevent suicide in patients with BD.^{2–4} However, a significant proportion of patients with BD experience relapse despite Li treatment.^{5,6} Overall, biomarkers predicting Li response are lacking and the mechanisms of Li action remain poorly understood. Little is known about the brain Li distribution or the brain regions in which Li exerts its therapeutic action. Moreover, although plasma Li concentrations have been shown to poorly

Jacques Stout and Anne-Sophie Hanak contributed equally to this study.

Abbreviations used: BD, bipolar disorder; BS, brainstem; CB, cerebellum; CPMG, Carr–Purcell–Meiboom–Gill; CSF, cerebrospinal fluid; CxF, frontal cortex; CxPO, parieto-occipital cortex; DE, diencephalon; FID, free induction decay; GM, gray matter; ICP-MS, inductively coupled plasma-mass spectrometry; MRI, magnetic resonance imaging; MRS, magnetic resonance spectroscopy; NMR, nuclear magnetic resonance; OB, olfactory bulbs; PFA, paraformaldehyde; RF, radiofrequency; ROI, region of interest; TSE, turbo-spin-echo; WM, white matter

predict the therapeutic effects and risk of non-response or relapse in humans, brain Li concentrations, if available, could represent a more accurate tool.⁷

Lithium-7 nuclear magnetic resonance (⁷Li-NMR) allows the non-invasive determination of brain Li concentrations and regional distribution.⁸ So far, ⁷Li-NMR studies in animals and humans^{7,9-20} have indicated that brain Li distribution is uneven and have suggested that the therapeutic response may be associated with altered transport of Li across the blood-brain barrier. However, the spatial resolution and precision of brain imaging have been limited by the expected low Li concentrations in the brain at therapeutic plasma concentrations (0.6–1.2 mmol/L) in patients and animal models. We designed the following experimental study: (i) to set up a three-dimensional lithium-7 magnetic resonance imaging (⁷Li MRI) protocol at 17.2 T and (ii) to conduct an initial *ex vivo* study of the brain Li distribution at therapeutic doses in chronically treated rats. As our initial lithium-7 magnetic resonance spectroscopy (⁷Li MRS)/MRI study, we chose to work on *ex vivo* rat heads and to validate our data by comparison with Li concentrations determined using inductively coupled plasma-mass spectrometry (ICP-MS).

2 | MATERIALS AND METHODS

Experiments were carried out within the ethical guidelines established by the National Institute of Health and the French Ministry of Agriculture. Protocols were approved by the Paris-Descartes University ethics committee for animal experimentation (project number: 2016050322008408).

2.1 | Animals

We used 6-week-old male Sprague-Dawley rats (Janvier, France), weighing 200–250 g at the start of the experiment. Animals were housed for 7 days before experimentation in an environment maintained at 20 ± 1°C with controlled humidity and light-dark cycle (lights on between 07:00 and 19:00 h). Food and water were provided *ad libitum*.

2.2 | Chemicals and drugs

Lithium carbonate (Li₂CO₃) was purchased from Sigma-Aldrich (Saint-Quentin Fallavier, France) and diluted in tap water to obtain 800 and 1200 mg/L solutions. Paraformaldehyde (PFA) was purchased from Electron Microscopy Sciences (Hatfield, PA, USA), dissolved in phosphate buffer to obtain a 4% solution and filtered 24 h before the experiment.

2.3 | Li treatment and brain preparation

Rats were randomized into two groups, placed in individual cages and provided with drinking water containing Li₂CO₃ at 800 mg/L (*n* = 4) or 1200 mg/L (*n* = 6) for 28 days. The 800 mg/L dosage regimen has been reported previously to lead to plasma Li concentrations at the lower limit of the therapeutic range recommended in humans.²¹ Thus, to reach the upper limit, we chose to increase the Li₂CO₃ concentration to 1200 mg/L in drinking water. To allow blood and brain sampling, rats were anesthetized on day 28 in an induction chamber (Minerve, France) with 4% isoflurane (Vetflurane®, Virbac, France) during 5 min, followed by 2% isoflurane delivered by a mask. Blood samples (100 µL) were collected from the femoral vein in Eppendorf tubes containing 10 µL of sodium heparin (Choay®, Sanofi Winthrop, France). Plasma and erythrocytes were separated by centrifugation at 1957 g during 10 min and stored until analysis at –20°C and +4°C, respectively. Thereafter, rats underwent exsanguination to eliminate residual blood from the brain by intracardiac infusion of 0.9% NaCl. Brain fixation was performed with 4% PFA administered at 15–21 mL/min during 5 min by the intracardiac route. Rats were decapitated. Their heads were immersed in 4% PFA and kept for 24 h at +4°C until brain MRI study. Thereafter, the brains were carefully removed from the skull and sectioned into six separate fragments: olfactory bulbs (OB), frontal cortex (CxF), parieto-occipital cortex (CxPO), diencephalon (DE), cerebellum (CB) and brainstem (BS), as reported previously.²¹ Brain samples were dried in an oven at +80°C overnight, weighed, digested in nitric acid (10 µL/mg of dry tissue) and heated for 1–2 h at +70°C. MilliQ water was added to obtain a solution of 10 g/L of dry tissue. Plasma, erythrocyte and brain Li contents were quantified using ICP-MS (Elan DRCe Perkin Elmer, Courtaboeuf, France) by standard addition calibration, as reported previously.²¹ Table 1 summarizes the dry-to-wet matter ratios used to convert ICP-MS concentrations into µmol/g wet.

TABLE 1 Dry-to-wet matter ratio for the different rat brain regions of interest

Brain area	Ratio
Olfactory bulb	0.166
Frontal cortex	0.196
Parieto-occipital cortex	0.210
Diencephalon	0.239
Cerebellum	0.206
Brainstem	0.288

2.4 | Li *ex vivo* wash-out experiment

In order to assess the wash-out of Li from our *ex vivo* rats, two rats were administered an acute intraperitoneal dose of Li_2CO_3 (185 mg/kg),²¹ 6 h prior to PFA fixation of their brains. One rat head was kept intact, and the other rat brain was extracted from the skull. Both were immersed in 4% PFA and samples were analyzed after 24 h, 48 h, 1, 2 and 3 weeks using ICP-MS to follow the Li concentration in the respective PFA bath.

2.5 | ^7Li -NMR measurements

^7Li -NMR data were acquired on a horizontal 17.2-T MRI scanner (Biospec, Bruker BioSpin, Ettlingen, Germany). A home-built dual-resonance $^1\text{H}/^7\text{Li}$ surface coil was built for this study consisting of two co-planar loops corresponding to ^7Li (diameter, 38 mm; operating frequency, 283.78 MHz) and ^1H (diameter, 24 mm; operating frequency, 730.20 MHz) channels, respectively. Each rat head was lodged in a Falcon 50-mL tube (Fisher Scientific, Villebon-sur-Yvette, France), the remainder of the tube being filled with Fluorinert FC40 (3 M, Electronic Liquids, St Paul, MN, USA), a perfluorocarbonated oil commonly used in *ex vivo* MRI to eliminate the background ^1H signal and minimize susceptibility artifacts. Except for minor shifts, all rat heads were placed in the same position relative to the dual $^1\text{H}/^7\text{Li}$ radiofrequency coil to facilitate our Li quantification procedure.

For anatomical reference, a three-dimensional T_2^* -weighted ^1H image (multi-gradient-echo sequence; TE/TR = 3/300 ms; inter-echo, 4 ms; six echoes; resolution, $150 \times 150 \times 150 \mu\text{m}^3$) was acquired covering the entire brain.

After the acquisition of a few non-localized free induction decay (FID) spectra for calibration of the ^7Li channel reference power (TR = 4000 ms; bandwidth, 4 kHz; 16 averages), a three-dimensional T_2 -weighted ^7Li image was acquired [turbo spin-echo (TSE) sequence; TE/TR = 12/4000 ms; inter-echo, 12 ms; turbo-factor, 8; resolution, $2 \times 2 \times 4 \text{ mm}^3$; 1024 averages] for 36 h.

The T_2 and T_1 relaxation times of ^7Li were investigated using a Carr–Purcell–Meiboom–Gill (CPMG) sequence (TE/TR = 12/4000 ms; inter-echo, 12 ms; 24 echoes; bandwidth, 4 kHz; 128 averages) and a progressive saturation approach (TR = 0.4, 1, 2, 4, 10, 20 and 40 s; spectral bandwidth, 4 kHz; 16–160 averages) in eight and four rats out of 10, respectively.

2.6 | Relaxation time estimation

Following the integration of the ^7Li spectra, individual T_2 relaxation curves were normalized, averaged and fitted to both mono-exponential and bi-exponential functions, whereas the T_1 relaxation curve was fitted solely to a mono-exponential function. All fits were performed using Matlab (Mathworks, Natick, MA, USA) and a non-weighted Levenberg–Marquardt algorithm, yielding average relaxation times. In addition to the fast and slow relaxation times corresponding to the pools of bound and free Li cations, their respective volume fractions were estimated.¹⁷

2.7 | Image analysis

^7Li TSE data were reconstructed using a home-built Matlab (MathWorks) program. Figure 1 illustrates the different steps of our Li quantification pipeline based on a modified phantom replacement approach.²² The phantom replacement approach allows the estimation of the concentration map $[X(r)]$ of a sample from the comparison of its image $I(r)$ with the image $I_{\text{ref}}(r)$ of a phantom of known concentration $[Y]$:

$$[X(r)] = I(r) / I_{\text{ref}}(r) \cdot [Y]$$

For the same MRI sequence and acquisition parameters, the signal intensity depends on the effective B_1^+ and B_1^- fields, as well as the T_1 and T_2 relaxation times of the sample or the reference phantom. If one were to assume an identical positioning and coil loading with our rat heads and reference phantom, the knowledge of their respective T_1 and T_2 weighting should be sufficient to calculate $[X(r)]$.

As a reference, a 50-mL Li gel phantom (10 mmol/L in 4% agarose) was used. Identical radiofrequency (RF) coil positioning and sequence parameters were used for the acquisition of the reference three-dimensional T_2 -weighted ^7Li image and T_2 - and T_1 -weighted spectra.

For all animals, the anatomical images were aligned together by co-registration to a home-built rat brain anatomical template using SPM8 (Figure 1A–D). This high-resolution template (isotropic voxels, 90 μm) was created using 16 *ex vivo* T_2^* -weighted ^1H MR images acquired at 7 T from 16 control rats (Fisher 344, Charles River, France). The same transformations were applied to each ^7Li MR image (Figure 1B–E). Then, each T_2 -weighted image was segmented into probability maps of gray matter (GM), white matter (WM) and cerebrospinal fluid (CSF) using the SPM8 unified segmentation approach²³ and rat brain tissue priors provided by Valdés-Hernández et al.²⁴ Thereafter, individual brain masks were calculated from the combination of the GM, WM and CSF probability maps using SPM8 (<http://www.fil.ion.ucl.ac.uk>).²⁵

For each experiment, a careful co-registration of the reference *in vitro* ^7Li image to the raw *ex vivo* ^7Li image was performed, followed by the application of the transformation towards the template referential (Figure 1C–F). The previously created mask was then applied to the reference ^7Li image. Using a Matlab script, the masked reference image was then fitted using a tenth degree polynomial three-dimensional function (Figure 1F, G). This allowed us to correct for the inhomogeneous excitation and reception profiles by calculating a ‘calibrated’ ^7Li brain image (Figure 1E–H), as the raw ^7Li *ex vivo* brain image divided by the mathematical model of the reference ^7Li image. To account for the differential T_1 and T_2 weighting between our *ex vivo* acquisitions and the reference ^7Li image, a correction factor of 1.33 was applied at this stage.

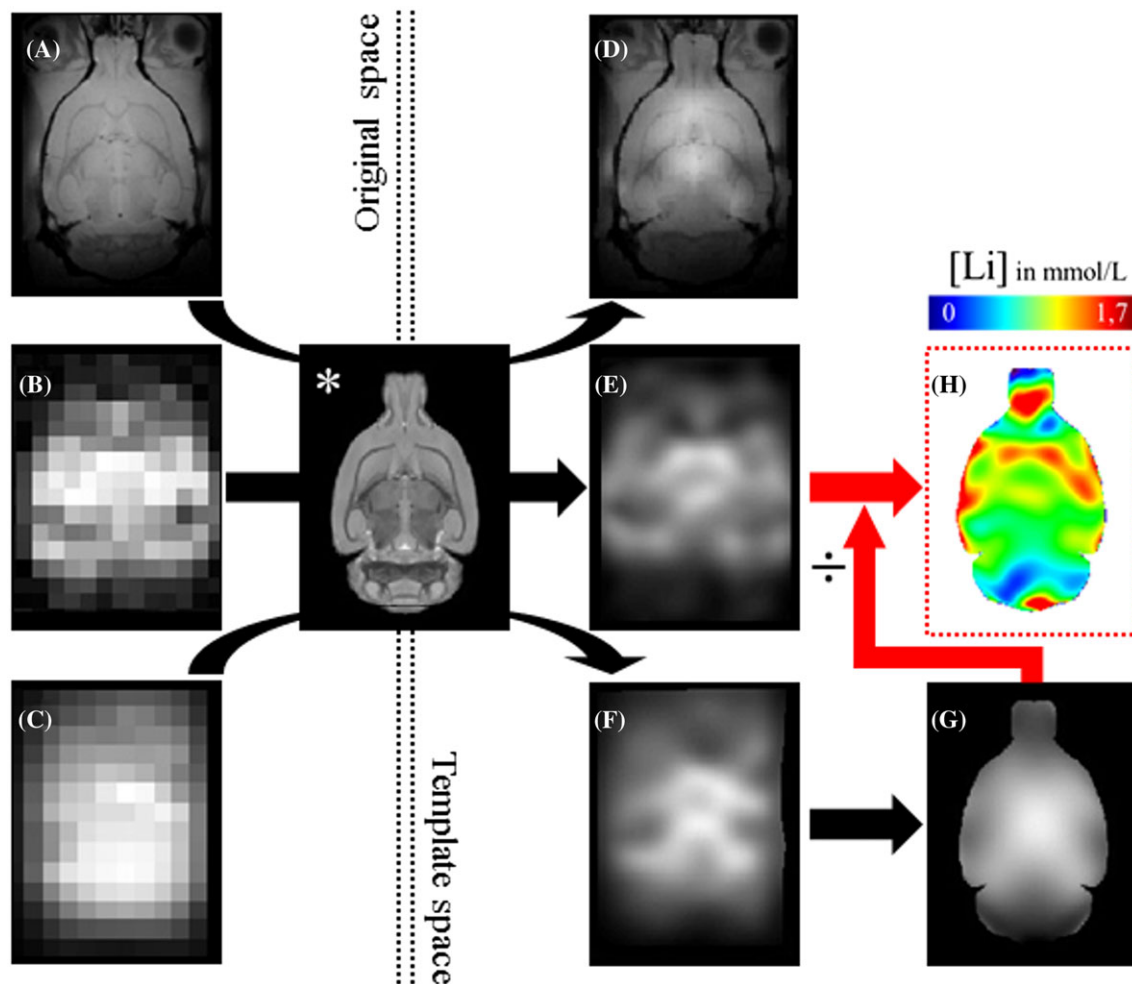


FIGURE 1 ^7Li magnetic resonance imaging (MRI) quantification pipeline using a modified phantom replacement approach. A, *Ex vivo* T_2^* -weighted anatomical reference. B, *Ex vivo* T_2 -weighted raw ^7Li MR image. C, *In vitro* T_2 -weighted ^7Li MR image of our 10 mmol/L Li gel phantom. D–F, images after co-registration to our home-built rat brain anatomical template (*). G, tenth degree polynomial interpolation of (F) and (H) 'calibrated' ^7Li MR images (in mmol/L) in the template space after brain masking. Starting from the co-registration step, all ^7Li MR images were interpolated at the resolution of the anatomic reference for visualization

For our region of interest (ROI)-based analysis, we applied, on each individual tissue class image, a DARTEL approach,²⁶ which is an automated, unbiased and non-linear atlas-building algorithm. As this atlas was defined upon its creation with 260 different ROI masks either from Valdés-Hernández et al.²⁴ (<http://www.idac.tohoku.ac.jp>) or the Waxholm atlas (<http://software.incf.org/>), we combined these so as to produce masks corresponding to our six dissected ROIs. For each rat, average ^7Li concentrations were calculated over each ROI. The ventral tier of the brain was not considered either for our ROI analysis or the ICP-MS dosages. Lastly, our brain Li concentration maps (in the template referential) were scaled to a whole-brain mean of unity and these ten normalized brain Li distributions were averaged.

3 | RESULTS

3.1 | Non-localized ^7Li T_1 and T_2 relaxation times

The longitudinal and transverse relaxation decays of ^7Li in the *ex vivo* rat heads and gel phantom at 17.2 T are plotted in Figure 2, together with their respective exponential fits. For the *ex vivo* rat heads, spin–spin relaxation times $T_{2,\text{slow}}$ and $T_{2,\text{fast}}$ were 369 ms (27%) and 44 ms (73%), whereas $T_{2,\text{mono}}$ was 128 ms. For the gel phantom, $T_{2,\text{slow}}$ and $T_{2,\text{fast}}$ were 404 ms (73%) and 53 ms (27%), whereas $T_{2,\text{mono}}$ was 298 ms. The longitudinal relaxation times $T_{1,\text{mono}}$ were 2014 ms for the *ex vivo* rat heads and 2280 ms for the gel phantom.

3.2 | Three-dimensional ^7Li MRI

As illustrated by Figure 1, ^7Li MRI exhibited a rather good sensitivity despite the modest brain Li content, the maximum normalized signal-to-noise ratio being estimated as $4.2 \times 10^7 \text{ mol}^{-1} \text{ min}^{-1/2}$. Therefore, the sensitivity threshold for a pixel (volume of 16 μL) using our T_2 -weighted ^7Li MRI

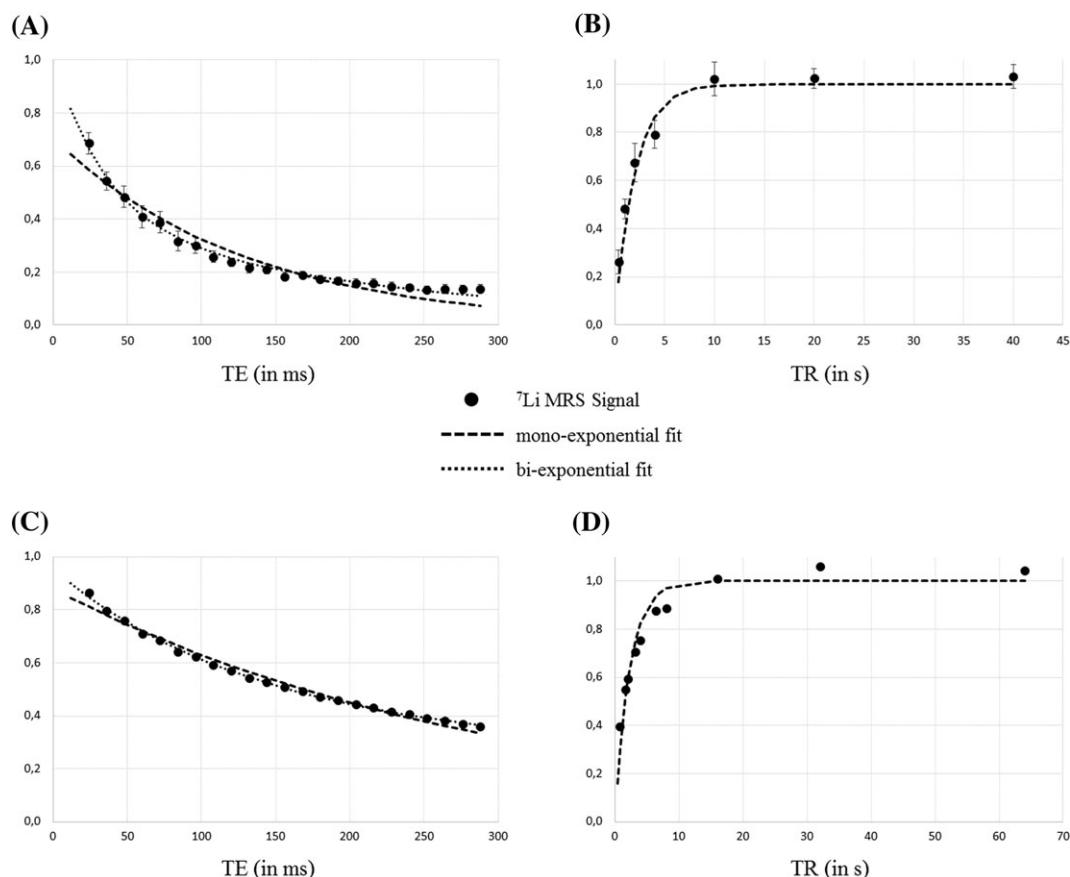


FIGURE 2 Normalized spin–spin and spin–lattice relaxation curves for lithium-7 (black dots) as a function of the echo time (TE) (a, average ${}^7\text{Li}$ magnetization from eight of ten *ex vivo* rat heads; C, *in vitro*) and repetition time (TR) (B, ${}^7\text{Li}$ magnetization from four of ten *ex vivo* rat heads; D, *in vitro*) and their exponential fits

sequence was 0.03 mmol/L at best. This sensitivity threshold was degraded to slightly above 0.1 mmol/L at the edge of the brain as a result of the inhomogeneous B_1^+ and B_1^- fields of our surface coil. Concretely, the average signal-to-noise ratio for our individual three-dimensional ${}^7\text{Li}$ MR images ranged from 3 to 38.

3.3 | Comparison between ${}^7\text{Li}$ MRI and ICP-MS measurements

As illustrated in Figure 3B, our MRI-derived brain Li concentrations matched with the ICP-MS measurements ($[\text{Li}]_{\text{MRI}} = 1.18[\text{Li}]_{\text{MS}}$, $R = 0.95$), demonstrating that our quantification approach efficiently corrected for most of the coil inhomogeneities and differential T_1 and T_2 weighting between *ex vivo* and reference ${}^7\text{Li}$ data. Table 2 summarizes the normalized Li concentrations in each brain ROI obtained using either ${}^7\text{Li}$ MRI or ICP-MS. Brain Li concentrations were consistently lower in the metencephalon (cerebellum and brainstem) and higher in the cortex. As shown in Figure 4, the averaged Li distribution (mean, $n = 10$) was largely heterogeneous, with normalized Li levels ranging from 0.84 to 1.14 across our ROIs (Table 2). As detailed in Table 2, the average brain-to-plasma Li ratio was 0.34 ± 0.04 , ranging from 0.29 to 0.39. Brain Li concentrations were reasonably correlated with plasma Li concentrations, Pearson correlation factors ranging from 0.63 to 0.90.

3.4 | Li *ex vivo* wash-out

Increasing Li concentrations were observed in the PFA bath of the whole rat head (up to 0.43 mmol/L at week 3), whereas the Li concentrations in the PFA bath containing the excised rat brain remained below 0.01 mmol/L despite the toxic levels of Li within both rats.

4 | DISCUSSION

In this study, we established a three-dimensional ${}^7\text{Li}$ MRI protocol at 17.2 T and conducted an initial *ex vivo* brain Li distribution study in chronically Li-treated rats using therapeutic dosage regimens. Our results were in agreement with previous studies using either ${}^7\text{Li}$ NMR^{12,13,15,16,18} or other analysis techniques, such as atomic absorption spectroscopy^{27,28} or radiographic dielectric track registration.²⁹ As illustrated in Figure 4, Li was unevenly distributed throughout the brain (from 0.4 to 1.4), with consistently lower concentrations in the metencephalon and higher concentrations in the cortex, mostly near the somatosensory areas. The distribution was largely symmetrical. Interestingly, low Li concentrations were also

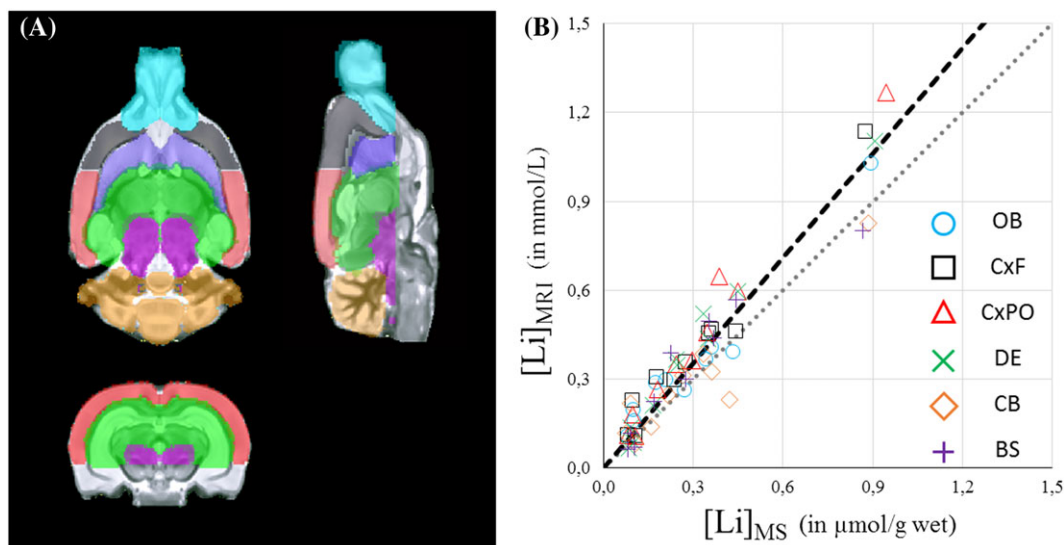


FIGURE 3 A, masks corresponding to our six dissected regions of interest. B, comparison of Li concentrations measured using ^7Li magnetic resonance imaging (MRI) (in mmol/L) versus inductively coupled plasma-mass spectrometry (ICP-MS) (in $\mu\text{mol/g}$ wet). Li concentrations from each dissected brain area are represented by distinct symbols. Overall, our quantification approach allowed us to match the ICP-MS values (Pearson correlation factor $R = 0.95$) with an average error of 18%. OB (blue), olfactory bulb; CxF (black), frontal cortex; CxPO (red), parieto-occipital cortex; DE (green), diencephalon; CB (brown), cerebellum; BS (violet), brainstem

TABLE 2 Normalized brain lithium (Li) distribution from inductively coupled plasma-mass spectrometry (ICP-MS) (wet matter) and ^7Li magnetic resonance imaging (MRI), Pearson correlation factor for each considered brain area and tissue-to-plasma ratio (mean \pm SD, $n = 10$)

Brain area	^7Li MRI	ICP-MS (wet)	Tissue-to-plasma ratio	R (Pearson)
Olfactory bulb	1.02 ± 0.24	1.00 ± 0.04	0.36 ± 0.19	0.63
Frontal cortex	1.09 ± 0.12	1.01 ± 0.02	0.39 ± 0.20	0.69
Parieto-occipital cortex	1.14 ± 0.13	1.04 ± 0.03	0.39 ± 0.16	0.74
Diencephalon	0.98 ± 0.17	0.99 ± 0.05	0.32 ± 0.11	0.81
Cerebellum	0.84 ± 0.25	0.97 ± 0.03	0.30 ± 0.19	0.65
Brainstem	0.91 ± 0.20	0.99 ± 0.02	0.29 ± 0.09	0.90

observed in the vicinity of the lateral ventricles. These observations are quite consistent with the hypothesis that transport mechanisms across the blood-brain and blood-CSF barriers may be responsible for the heterogeneity in brain Li distribution depending on the regional expression and activity of Na^+ exchangers.³⁰

Overall, ^7Li NMR-derived brain Li concentrations were nicely correlated with the brain Li concentrations measured by ICP-MS ($R = 0.95$). However, an average discrepancy of 18% was observed between the two techniques. In the past, such a correlation was established by Komoroski et al.¹⁶ between atomic absorption spectrophotometry and high-resolution ^7Li NMR spectroscopy with a comparable precision. Quantification errors were not homogeneous across ROIs, with errors of +34% (CxPO) to -17% (CB) being observed. Two hypotheses may explain these findings. First, our quantification pipeline relies on a three-dimensional polynomial model of a reference image to correct for both B_1^+ and B_1^- field inhomogeneities. Thus, Li content may have been overestimated for the ROIs closer to the RF coil and underestimated for the more distant ROIs. Second, the ICP-MS-derived brain Li concentrations were obtained after conversion from concentrations in dry matter assuming constant dry-to-wet matter ratio for each ROI (Table 1). As these ratios were determined from a separate group of rat brains, we cannot rule out discrepancies between rat brains, especially in relation to varying degrees of dehydration following tissue fixation using PFA.

As summarized in Table 2, brain Li concentrations were reasonably correlated with plasma Li concentrations (ranging from 0.63 to 0.90), yielding tissue-to-plasma Li ratios ranging from 0.29 (BS) to 0.39 (CxF and CxPO). Such correlations have been repeatedly reported in previous studies,³¹⁻³⁴ with most brain-to-plasma Li ratios ranging from 0.5 to 0.8. However, on an individual basis, plasma Li concentrations remain a poor indicator of brain Li levels in patients with BD because of various factors, including the Li dosage, co-medications and compliance,³⁴ as well as its different pharmacokinetics in plasma and the brain.^{21,31,35}

The investigation of PFA-fixed brain is a major limitation of this study. First, higher brain-to-plasma ratios should have been expected; the leaching of Li from our rat brain is a probable explanation for this discrepancy. Our hypotheses were as follows: (i) the 4% PFA infusion (and exsanguination) of our rat brains could have led to the complete or partial wash-out of the Li contained in the extracellular/interstitial compartment; or (ii) Li diffused from the *ex vivo* rat brain into its PFA fixation bath. Based on our observation of an insignificant wash-out of Li from an *ex vivo* PFA-fixed

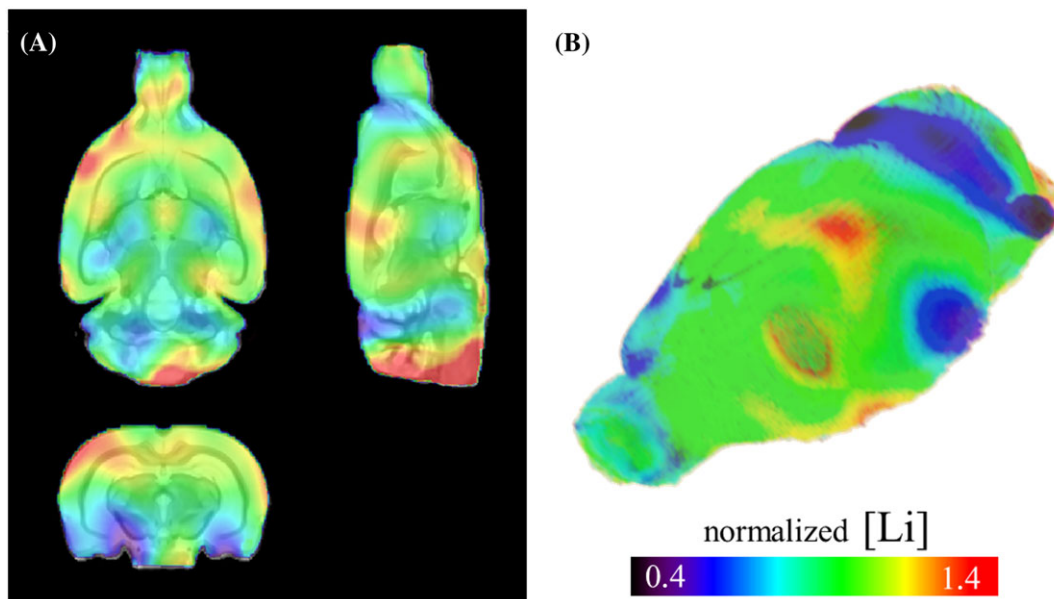


FIGURE 4 Normalized Li distribution in the rat brain *ex vivo* (mean, $n = 10$). A, orthogonal views co-registered with our home-built rat brain template. B, three-dimensional rendering. Except for some calibration errors at the fringes of the brain, Li is more concentrated in the cortex (notably the somatosensory cortex) and least concentrated in the metencephalon, as reported in previous studies. Interestingly, low Li concentrations are also observed close to the lateral ventricles

excised brain into its PFA bath, we can reasonably exclude this second hypothesis. With regard to our first hypothesis, the extracellular Li fraction was estimated to be 46% in the rat brain *in vivo*.¹⁷ Thus, the complete wash-out of the extracellular Li could halve the brain-to-plasma ratios *ex vivo*. Interestingly, the application of the same approach as Komoroski et al.¹⁷ to our *ex vivo* bi-exponential T_2 relaxation decays (Figure 2A) would achieve an extracellular Li fraction of 26%. This extracellular (or rather free) Li may be interpreted as the remainder of the 46% reported *in vivo*, meaning that about 60% would have been washed out by our PFA infusion. As a consequence, our data would rather reflect the intracellular Li distribution, justifying our lower than expected brain-to-plasma Li ratios. Second, we did not control for the risk of an intracerebral diffusion of Li. As such a phenomenon would lead to the redistribution of Li within the brain, our *ex vivo* Li distribution should be considered with caution.

As ^7Li NMR spectra present a single resonance, the use of a conventional imaging sequence may be advantageous compared with a chemical shift imaging sequence. Ultra-short TE sequences have also been proposed³⁶ to image ^7Li in patients with BD. This approach is appropriate for nuclei such as ^{23}Na or ^{17}O with short relaxation times. However, in the rat brain *ex vivo*, ^7Li exhibits much longer T_1 and T_2 relaxation times. Consequently, a TSE sequence seemed more fitting, as a decent percentage of each TR could be spent acquiring signal whilst limiting the T_1 weighting. Based on this initial study and our promising results, we are planning to improve our imaging protocol by increasing the turbo-factor and decreasing TR at the cost of a much higher duty cycle for our RF coil. Using a smaller quadrature coil should also be considered as an axis for improvement. Even more enticing would be the prospect of using a cryogenic RF coil.³⁷ Such a coil has already demonstrated a four-fold sensitivity gain at 9.4 T for ^{13}C MRS,³⁸ opening up the way to *ex vivo* ^7Li MRI at a resolution of 4 $\mu\text{L}/\text{pixel}$ or an *in vivo* ^7Li MRI study in rodents without compromising either sensitivity or spatial resolution.

Finally, this study should be considered as a stepping stone towards *in vivo* ^7Li MRI in rodents with several potential implications. We strongly believe that combining ^7Li MRI with anatomical, structural and functional ^1H MRI will help to elucidate the mood-stabilizing action of Li, as well as to assess potential additional therapeutic benefits in the increasingly available rodent models of psychiatric diseases or conditions, including aggression, depression, circadian rhythms, schizophrenia and tardive dyskinesia.³⁹ More generally, it opens up avenues for future developments of this technique in Li-treated patients with BD to better explore: (i) brain Li pharmacokinetics in treated patients; (ii) the links between brain Li distribution and response (both therapeutic and side effects); and (iii) the Li mechanism of action which remains unknown.

5 | CONCLUSION

To the best of our knowledge, this study is the first comprehensive report on brain Li distribution using quantitative ^7Li MRI in rats. Compared with previous studies using analysis techniques, such as radiographic dielectric track registration, atomic absorption and mass spectroscopy,^{21,27-30} our NMR approach allows a quantitative and retrospective exploration of brain Li distribution without any extensive tissue manipulation or precise dissection. In the future, further technical developments should help us to achieve better spatial or temporal resolutions, opening up the way for more ambitious studies to better understand Li pharmacodynamics, as well as its biological action, in animal models, particularly its therapeutic actions in affective disorders and suicidal behaviors in humans.

ACKNOWLEDGEMENTS

The authors thank Dr Michel Luong and Edouard Chazel for the $^7\text{Li}/^1\text{H}$ radiofrequency coil, Drs Sébastien Mériaux and Luisa Ciobanu for helpful discussions, and Professor Denis Le Bihan for his support. This work was funded by IDEX Université Sorbonne-Paris-Cité research call (RespoLi project 2013, PI: Frank Bellivier) and the French National Research Agency (BIP-Li7 project 2014, ANR-14-CE15-0003-01, PI: Frank Bellivier).

REFERENCES

1. Das Gupta R, Guest JF. Annual cost of bipolar disorder to UK society. *Br J Psychiatry*. 2002;180:227-233.
2. Maj M. The effect of lithium in bipolar disorder: A review of recent research evidence. *Bipolar Disord*. 2003;5:180-188.
3. Baldessarini RJ, Tondo L, Davis P, Pompili M, Goodwin FK, Hennen J. Decreased risk of suicides and attempts during long-term lithium treatment: A meta-analytic review. *Bipolar Disord*. 2006;8:625-639.
4. Cipriani A, Hawton K, Stockton S, Geddes JR. Lithium in the prevention of suicide in mood disorders: Updated systematic review and meta-analysis. *Br Med J*. 2013;346:f3646
5. Price LH, Heninger GR. Lithium in the treatment of mood disorders. *N Engl J Med*. 1994;331:591-598.
6. Maj M, Pirozzi R, Magliano L. Nonresponse to reinstated lithium prophylaxis in previously responsive bipolar patients: Prevalence and predictors. *Am J Psychiatry*. 1995;152:1810-1811.
7. Machado-Vieira R, Otaduy MC, Zanetti MV, et al. A selective association between central and peripheral lithium levels in remitters in bipolar depression: A 3T-(7) li magnetic resonance spectroscopy study. *Acta Psychiatr Scand*. 2016;133:214-220.
8. Komoroski RA. Biomedical applications of ^7Li NMR. *NMR Biomed*. 2005;18:67-73.
9. Renshaw PF, Haselgrove JC, Leigh JS, Chance B. In vivo nuclear magnetic resonance imaging of lithium. *Magn Reson Med*. 1985;2:512-516.
10. Renshaw PF, Haselgrove JC, Bolinger L, Chance B, Leigh JS Jr. Relaxation and imaging of lithium in vivo. *Magn Reson Imaging*. 1986;4:193-198.
11. Ramaprasad S, Newton JE, Cardwell D, Fowler AH, Komoroski RA. In vivo ^7Li NMR imaging and localized spectroscopy of rat brain. *Magn Reson Med*. 1992;25:308-318.
12. Ramaprasad S. Lithium spectroscopic imaging of rat brain at therapeutic doses. *Magn Reson Imaging*. 2004;22:727-734.
13. Ramaprasad S, Ripp E, Pi J, Lyon M. Pharmacokinetics of lithium in rat brain regions by spectroscopic imaging. *Magn Reson Imaging*. 2005;23:859-863.
14. Komoroski RA, Newton JE, Sprigg JR, Cardwell D, Mohanakrishnan P, Karson CN. In vivo ^7Li nuclear magnetic resonance study of lithium pharmacokinetics and chemical shift imaging in psychiatric patients. *Psychiatry Res*. 1993;50:67-76.
15. Komoroski RA, Pearce JM, Newton JE. The distribution of lithium in rat brain and muscle in vivo by ^7Li NMR imaging. *Magn Reson Med*. 1997a;38:275-278.
16. Komoroski RA, Pearce JM, Newton JEO. Distribution of lithium in rat brain and muscle by ^7Li NMR and atomic absorption spectrophotometry in vitro. *J Magn Reson Anal*. 1997b;3:169-174.
17. Komoroski RA, Pearce JM. Estimating intracellular lithium in brain in vivo by localized ^7Li magnetic resonance spectroscopy. *Magn Reson Med*. 2008;60:21-26.
18. Komoroski RA, Lindquist DM, Pearce JM. Lithium compartmentation in brain by ^7Li MRS: Effect of total lithium concentration. *NMR Biomed*. 2013;26:1152-1157.
19. Lee JH, Adler C, Norris M, et al. 4-T ^7Li 3D MR spectroscopy imaging in the brains of bipolar disorder subjects. *Magn Reson Med*. 2012;68:363-368.
20. Port JD, Rampton KE, Shu Y, Manduca A, Frye MA. Short TE (7) Li-MRS confirms bi-exponential lithium T2 relaxation in humans and clearly delineates two patient subtypes. *J Magn Reson Imaging*. 2013;37:1451-1459.
21. Hanak AS, Chevillard L, El Balkhi S, Risède P, Peoc'h K, Mégarbane B. Study of blood and brain lithium pharmacokinetics in the rat according to three different modalities of poisoning. *Toxicol Sci*. 2015;143:185-195.
22. Soher BJ, van Zijl PC, Duyn JH, Barker PB. Quantitative proton MR spectroscopic imaging of the human brain. *Magn Reson Med*. 1996;35:356-363.
23. Ashburner J, Friston KJ. Unified segmentation. *Neuroimage*. 2005;26:839-851.
24. Valdés-Hernández PA, Sumiyoshi A, Nonaka H, et al. An in vivo MRI template set for morphometry, tissue segmentation, and fMRI localization in rats. *Front Neuroinform*. 2011;5:26
25. Friston KJ, Ashburner J, Frith CD, Poline JB, Heather JD, Frackowiak RS. Spatial registration and normalization of images. *Hum Brain Mapp*. 1995;3:165-189.
26. Ashburner J. A fast diffeomorphic image registration algorithm. *Neuroimage*. 2007;38:95-113.
27. Mukherjee BP, Bailey PT, Pradhan SN. Temporal and regional differences in brain concentrations of lithium in rats. *Psychopharmacology (Berl)*. 1976;48:119-121.
28. Nelson SC, Herman MM, Bensch KG, Barchas JD. Localization and quantitation of lithium in rat tissue following intraperitoneal injections of lithium chloride. *II Brain J Pharmacol Exp Ther*. 1980;212:11-15.
29. Sandner G, Di Scala G, Oberling P, Abbe JC, Stampfler A, Sens JC. Distribution of lithium in the rat brain after a single administration known to elicit aversive effects. *Neurosci Lett*. 1994;166:1-4.
30. Ebadi MS, Simmons VJ, Hendrickson MJ, Lacy PS. Pharmacokinetics of lithium and its regional distribution in rat brain. *Eur J Pharmacol*. 1974;27:324-329.
31. Ebara T, Smith DF. Lithium levels in blood platelets, serum, red blood cells and brain regions in rats given acute or chronic lithium salt treatments. *J Psychiatr Res*. 1979;15:183-188.
32. Sachs GS, Renshaw PF, Lafer B, et al. Variability of brain lithium levels during maintenance treatment: A magnetic resonance spectroscopy study. *Biol Psychiatry*. 1995;38:422-428.

33. Soares JC, Boada F, Spencer S, et al. Brain lithium concentrations in bipolar disorder patients: Preliminary ^7Li magnetic resonance studies at 3 T. *Biol Psychiatry*. 2001;49:437-443.
34. Pearce JM, Lyon M, Komoroski RA. Localized ^7Li MR spectroscopy: In vivo brain and serum concentrations in the rat. *Magn Reson Med*. 2004;52:1087-1092.
35. Hillert M, Zimmermann M, Klein J. Uptake of lithium into rat brain after acute and chronic administration. *Neurosci Lett*. 2012;521:62-66.
36. Boada FE, Qian Y, Gildengers A, Phillips M, Kupfer D. In vivo 3D lithium MRI of the human brain. *Proceedings of the 18th Annual Meeting ISMRM*, Stockholm, Sweden, 2010;592.
37. Darrasse L, Ginefri JC. Perspectives with cryogenic RF probes in biomedical MRI. *Biochimie*. 2003;85:915-937.
38. Sack M, Wetterling F, Sartorius A, Ende G, Weber-Fahr W. Signal-to-noise ratio of a mouse brain (^{13}C CryoProbe™ system in comparison with room temperature coils: Spectroscopic phantom and in vivo results. *NMR Biomed*. 2014;27:709-715.
39. O'Donnell KC, Gould TD. The behavioral actions of lithium in rodent models: Leads to develop novel therapeutics. *Neurosci Biobehav Rev*. 2007;31:932-962.

How to cite this article: Stout J, Hanak A-S, Chevillard L, et al. Investigation of lithium distribution in the rat brain *ex vivo* using lithium-7 magnetic resonance spectroscopy and imaging at 17.2 T. *NMR in Biomedicine*. 2017;30:e3770. <https://doi.org/10.1002/nbm.3770>